Minimal model for zero-inertia instabilities in shear-dominated non-Newtonian flows

S. Boi,[1] A. Mazzino,[2,3] and J. O. Pralits[2]
[1]*Physics Department, University of Genova, Via Dodecaneso 33, 16146 Genova, Italy*
[2]*DICCA, University of Genova, Via Montallegro 1, 16145 Genova, Italy*
[3]*INFN and CINFAI Consortium, Genova Section, Via Dodecaneso 33, 16146 Genova, Italy*
(Received 16 June 2013; published 12 September 2013)

The emergence of fluid instabilities in the relevant limit of vanishing fluid inertia (i.e., arbitrarily close to zero Reynolds number) has been investigated for the well-known Kolmogorov flow. The finite-time shear-induced order-disorder transition of the non-Newtonian microstructure and the corresponding viscosity change from lower to higher values are the crucial ingredients for the instabilities to emerge. The finite-time low-to-high viscosity change for increasing shear characterizes the rheopectic fluids. The instability does not emerge in shear-thinning or -thickening fluids where viscosity adjustment to local shear occurs instantaneously. The lack of instabilities arbitrarily close to zero Reynolds number is also observed for thixotropic fluids, in spite of the fact that the viscosity adjustment time to shear is finite as in rheopectic fluids. Renormalized perturbative expansions (multiple-scale expansions), energy-based arguments (on the linearized equations of motion), and numerical results (of suitable eigenvalue problems from the linear stability analysis) are the main tools leading to our conclusions. Our findings may have important consequences in all situations where purely hydrodynamic fluid instabilities or mixing are inhibited due to negligible inertia, as in microfluidic applications. To trigger mixing in these situations, suitable (not necessarily viscoelastic) non-Newtonian fluid solutions appear as a valid answer. Our results open interesting questions and challenges in the field of smart (fluid) materials.

DOI: 10.1103/PhysRevE.88.033007 PACS number(s): 47.51.+a, 47.27.−i

I. INTRODUCTION

Control of mixing in fluid environments with very low Reynolds numbers is a need of paramount importance for many practical purposes [1]. Applications range from biochemistry analysis in microfluidic devices [2], where mixing has to be rapid and efficient, to lab-on-a-chip applications, where mixing has to be reduced to avoid spurious effects as in microfluidic rheometer applications [3].

For small Reynolds numbers, the resulting flow of a Newtonian fluid is typically laminar, and mixing occurs via diffusion. This mechanism is, however, extremely inefficient and slow. Fortunately, in many low-Reynolds number applications, including microfluidics, fluids are viscoelastic (a form of non-Newtonianity), a fact that has been recognized as an enormous advantage with respect to Newtonian fluids for the possibility of generating mixing via purely elastic instabilities [4]. If properly triggered, these instabilities can originate the so-called elastic turbulence [5]. Elastic turbulence is characterized by the algebraic decay of velocity power spectra over a wide range of scales and by its ability to generate more efficient mixing than in an ordered flow.

Elastic instabilities and elastic turbulence are characteristics of viscoelastic fluids: long polymer molecules added to a fluid make it elastic and capable of storing stresses that depend on the history of deformation, thereby providing the fluid a memory. The streamline curvature was thought to be a necessary ingredient to trigger the instability via a balance between normal stresses and streamline curvature [6–8]. More recently, simple parallel flows clearly showed the emergence of purely elastic instabilities [9,10] and turbulence [11] even in the absence of curvature. Remarkably, the same class of viscoelastic parallel flows also displays other nontrivial viscoelastic properties including the well-known drag reduction by polymer additives [12,13].

Our aim here is to show that the existence of purely non-Newtonian instabilities (a prelude to mixing in the nonlinear stage) occurring arbitrarily close to zero Reynolds number also exist for non-Newtonian fluids which are not viscoelastic. Interesting discussions on the relationship between viscoelasticity and other forms of non-Netwonianity (including thixotropy and rheopecticity) can be found in Ref. [14]. The instabilities we have identified originate from the interplay between shear and order-disorder transitions associated with the non-Newtonian structure. Microstructural disorder is related to large shear and manifests itself at mesoscopic scales via a low-to-high-viscosity change. Such a change in the viscosity characterizes the so-called rheopectic fluids, which share with shear-thickening fluids the property that their apparent viscosities increase with strain. The crucial difference is that, for shear-thickening fluids, the response to strain is almost instantaneous while this is not so for rheopectic fluids. We found that this apparently innocent difference is the key point for purely non-Newtonian instabilities to emerge even for vanishing Reynolds numbers.

Our findings call for a thorough research in the field of smart fluid materials to maximize the rheological properties, here identified as crucial for instabilities and mixing to emerge, even for vanishing fluid inertia.

As a model of rheopectic fluids we modified, in a physically consistent way, the well-known and widely used Carreau-Bird model [15] in order to model a finite-time response of the apparent viscosity to shear. This property is here achieved in terms of a simple kinetic equation mimicking the unceasing order-disorder transition originated by the competition between network restoring forces and shear-induced network. With the term network we here denote collective behaviors, such as those originated in dense suspensions or by polymers in water when subjected to shear. Another relevant example is the transition from a flow of colloids (corresponding to a

low-viscosity state) to jamming of the colloids with formation of chains (corresponding to a high-viscosity state) [16].

For sufficiently large network relaxation times, the network acquires proper dynamics with characteristic times that can become comparable to those of the underlying flow. Under these conditions of strong coupling, nontrivial effects including network instabilities are expected. The investigation of this intriguing possibility is one of the main subjects of this paper.

II. THE NON-NEWTONIAN MODEL

Let us start from the definition of the static version of our non-Newtonian fluid. Here, static is used to emphasize that the fluid response to stresses takes place instantaneously. The next step will be to incorporate a finite time response of the fluid that, as we will show, will be the crucial ingredient for network instabilities to emerge.

A widely accepted model to describe the dependence on shear rates of the apparent viscosity is the so-called Carreau-Bird model [15]. According to this model, the expression for the viscosity is

$$\mu = \mu_\infty + (\mu_0 - \mu_\infty)(1 + 2a^2\dot{\gamma}^2)^{\frac{n-1}{2}}, \tag{1}$$

where $\dot{\gamma} \equiv (2e_{\alpha\beta}e_{\alpha\beta})^{1/2}$ is the strain rate, $e_{\alpha\beta} \equiv \frac{1}{2}(\partial_\alpha u_\beta + \partial_\beta u_\alpha)$ is the strain tensor, a is a constant, and n (not necessarily integer and $n < 1$ to model shear-thinning fluids) is a measure of how far different fluid properties are from a purely Newtonian fluid. Tensorial components α and β range from 1 to 2 and, as customary, we use the Einstein convention that repeated indices are implicitly summed over. The Newtonian limit is achieved for $n = 1$ and/or $a \to 0$. The physical meaning of $1/a$ is that of a threshold on the strain-rate $\dot{\gamma}$ above which the non-Newtonian character of the fluid smoothly emerges. The constant a is thus not related to a typical response time of the fluid to the strain.

The parameter μ_0 is the viscosity at zero shear rate (i.e., for $\dot{\gamma} \to 0$) and μ_∞ is the infinite-shear-rate viscosity (i.e., for $\dot{\gamma} \to \infty$). Taking n as an adjustable parameter, one can properly describe numerous non-Newtonian substances [17].

In many cases the infinite shear viscosity μ_∞ is negligible [18] and the model simplifies to

$$\mu = \mu_0(1 + 2a^2\dot{\gamma}^2)^{\frac{n-1}{2}}, \tag{2}$$

where only three free parameters are involved.

Despite the fact that the model was originally proposed to describe shear-thinning fluids, the currently available (limited) information on shear-thickening fluids suggests the use of Eq. (2) with $n > 1$ to describe this class of non-Newtonian fluids [17]. Notwithstanding the paucity of rheological data on such systems, it is not yet possible to say with confidence whether these materials also display limiting viscosities μ_0 and μ_∞. We nevertheless assume in the following, for the sake of continuity with the Newtonian case, the existence of a well-defined zero-shear-rate viscosity μ_0.

Let us now proceed to include a fluid finite time response to shear. The idea is to introduce a kinetic equation for a scalar structure parameter λ in the same spirit of thixotropic modeling [14] where such an equation is inspired by chemical kinetics.

The resulting kinetic equation here simply follows from the requirement that Eq. (2) must be obtained in the limit of fast network response. By imposing this constraint one has

$$\frac{d\lambda}{dt} = -\frac{\lambda}{\tau} + \frac{2\,a^2\dot{\gamma}^2}{\tau}, \tag{3}$$

where $\frac{d\lambda}{dt}$ is a material derivative. In the above equation, the steady state (ss) value of λ (λ^{ss}) follows from a balance between the rate for network build-up and breakdown. For a constant $\dot{\gamma}$, after a time τ one has $\lambda^{ss} = 2a^2\dot{\gamma}^2$.

To close the circuit it is necessary to assume a relationship between λ and the viscosity μ (i.e., a relationship between the structure and the flow). To obtain Eq. (2) at the stationary state, we assume the following relationship:

$$\mu = \mu_0(1 + \lambda)^{\frac{n-1}{2}}. \tag{4}$$

Note that for $n < 1$ the model describes the so-called thixotropic behavior; rheopectic behavior is captured by $n > 1$.

Once the stress tensor is expressed in the generalized Newtonian form, $\tau_{\alpha\beta} = 2\mu e_{\alpha\beta}$, the resulting governing equations read

$$\partial_t u_\alpha + \mathbf{u}\cdot\boldsymbol{\partial} u_\alpha = -\partial_\alpha p/\rho + \partial_\beta(\tau_{\alpha\beta})/\rho + f_\alpha, \tag{5}$$

$$\boldsymbol{\partial}\cdot\mathbf{u} = 0, \tag{6}$$

where $\boldsymbol{f}$ is a given volume force. The latter force is chosen here to excite the celebrated shear-dominated Kolmogorov parallel flow [19], here assumed in its two-dimensional form $\boldsymbol{U} = (U(y),0)$ with $U(y) = V\cos(y/L)$ and a uniform pressure P (which can be set to zero). The corresponding equilibrium expression for λ is $\Lambda = 2a^2(\partial_y U)^2$. $\boldsymbol{U}$, P, and Λ thus constitute the basic state of which the stability analysis will be studied in this paper.

The following dimensionless free parameters enter into play: $\mathrm{Re} = \rho V L/\mu_0$, $\mathrm{De} = \tau V/L$, and $\Gamma = aV/L$. The first one is the Reynolds number (in terms of the zero-shear-rate viscosity), while the second is analogous to the Deborah number for viscoelastic solutions. The network relaxation time τ towards an ordered state is indeed the analog of the Zimm relaxation time in dilute polymer solutions [15]. There, the ordered state corresponds to polymers in their coiled state and the disordered phase is associated with elongated polymers. Finally, Γ, sometimes called the Carreau number, is a measure of the level of how non-Newtonian a fluid is.

A relevant limiting case of the model is the one corresponding to $\mathrm{De} \equiv \Gamma$ [i.e., $a \equiv \tau$ in Eq. (3)]. For small De (i.e., fast network response) one recovers the Newtonian limit; this does not happen for small De when $\mathrm{De} \neq \Gamma$. By increasing De, the apparent viscosity increases proportionally to De^2 and non-Newtonian behavior becomes increasingly important. The growing importance of non-Newtonian effects is accompanied by the slowing down of the typical time associated with the network response. This phenomenon is expected to cause network instabilities like the purely elastic instabilities observed in dilute polymer solutions. We will address this important issue in the following.

III. LINEAR STABILITY ANALYSIS: NUMERICAL RESULTS

Let us now consider the linearized equations for the system of perturbations $(\boldsymbol{w},q,\sigma)$ of the basic state $(\boldsymbol{U},P,\Lambda)$. Equations (3), (5), and (6) become

$$\boldsymbol{\partial}\cdot\boldsymbol{w}=0, \tag{7}$$

$$\partial_t w_\alpha+\partial_\beta(U_\beta w_\alpha+w_\beta U_\alpha)=-\partial_\alpha q+\partial_\beta\tau'_{\alpha\beta}, \tag{8}$$

$$\partial_t\sigma+\partial_\beta(U_\beta\sigma+w_\beta\Lambda)=-\frac{\sigma}{\mathrm{De}}+\frac{8\Gamma^2E_{\alpha\beta}e'_{\alpha\beta}}{\mathrm{De}}, \tag{9}$$

where space coordinates, velocities, time, and pressure have been made dimensionless as customary in terms of L, V, and ρ. We have defined

$$\tau'_{\alpha\beta}=2\mu_b\,e'_{\alpha\beta}+2\mu' E_{\alpha\beta}, \tag{10}$$

where

$$\mu_b=\frac{(1+\Lambda)^{\frac{n-1}{2}}}{\mathrm{Re}},\quad \mu'=\frac{(1+\Lambda)^{\frac{n-3}{2}}(n-1)\sigma}{2\mathrm{Re}}. \tag{11}$$

Moreover, $e'_{\alpha\beta}$ and $E_{\alpha\beta}$ are the strain tensors based on the perturbations and the basic state, respectively.

The linear stability of the basic flow is analyzed assuming solutions of the form $(\boldsymbol{w},q,\sigma)=(\hat{\boldsymbol{w}},\hat{q},\hat{\sigma})\exp[ik(x-ct)]$, where k is the real-valued streamwise wave number and c is the complex-valued phase velocity. Equations (7)–(10) are recast in the form of a generalized eigenvalue problem where derivatives with respect to y are approximated using second-order finite differences and periodic boundary conditions are imposed. This constitutes a dispersion relation for $c(\mathrm{Re},\mathrm{De},\Gamma,k)$ where $\mathrm{Im}(c)>0$ identifies unstable solutions. The eigenvalue problem is numerically solved using the QZ algorithm [20] and the marginal curves are defined as solutions for which $\mathrm{Im}(c)=0$.

In the upper panel of Fig. 1 we show marginal curves in the parameter space Re-Γ for $n=1.3$ and different De. Below these curves we have stability; instabilities are found above the curves. $\mathrm{De}=0$ corresponds to the case of instantaneous response of the network. No network instabilities are observed in this case: the marginal curve increases with Γ as a power law (see inset) and it does not cross the $\mathrm{Re}=0$ axis. The situation drastically changes for finite De: depending on its value, marginal curves indeed cross the $\mathrm{Re}=0$ axis. This is the fingerprint of network instabilities. Although not shown, this property holds true for all $n>1$.

In the lower panel of Fig. 1 marginal curves are presented in the parameter space Re-De, again for $n=1.3$, and different values of Γ. In all cases, a critical De (as $\mathrm{Re}\to 0$) exists, whose value decreases for increasing Γ, associated with a transition to network instabilities. Once again, the key role of the finite-time response of the network to strain is crucial for network instabilities to emerge.

So far we have considered Γ and De as independent parameters. Let us now consider the limiting case of the model where the two parameters merge in a unique parameter, i.e., $\Gamma\equiv\mathrm{De}$. In Fig. 2 the resulting marginal curves are shown for different values of n. The emergence of network

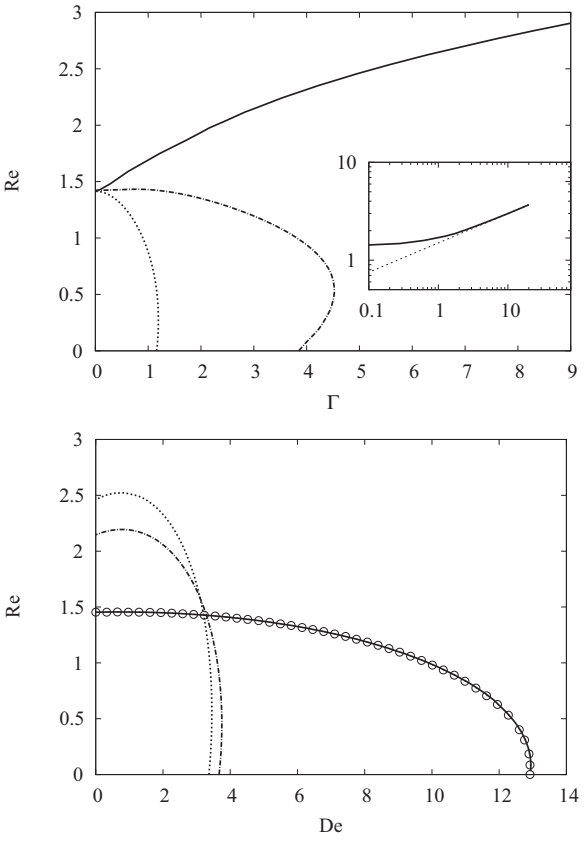

FIG. 1. Upper panel: Marginal curves in Re-Γ plane and $n=1.3$ for different values of De. Here, $\mathrm{De}=0$ (−), $\mathrm{De}=3.5$ (- · -) and $\mathrm{De}=5$ (· · ·). Inset: log-log plot for the case $\mathrm{De}=0$ (−) showing a power-law behavior (- -) with exponent ∼0.3 as $\Gamma\to\infty$. Lower panel : Marginal curves in the Re-De plane and $n=1.3$ for different values of Γ. Here, $\Gamma=0.3$ (−), $\Gamma=3$ (- · -), and $\Gamma=5$ (· · ·). The prediction from the multiple-scale expansion discussed in the final part of this article is shown with the symbol (○).

instability is observed but in this case the behavior is not monotonically decreasing toward $\mathrm{Re}=0$. A maximum exists for certain values of De (the larger n the smaller De at which

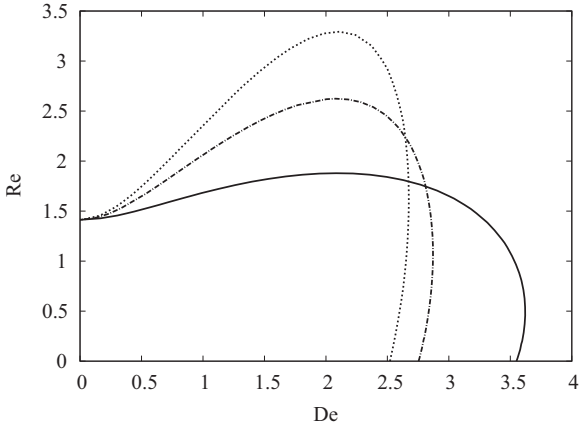

FIG. 2. Marginal curves in the Re-De plane with $\Gamma\equiv\mathrm{De}$, for different values of n. Here, $n=1.3$ (−), $n=1.7$ (- · -), and $n=2$ (· · ·).

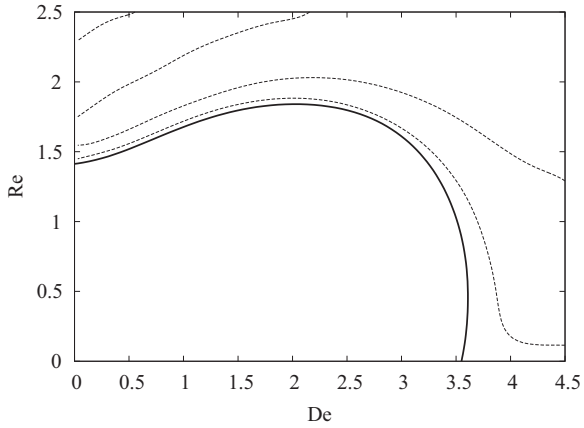

FIG. 3. Wave number k of least stable mode in Re-De plane with $\Gamma \equiv \mathrm{De}$ and $n = 1.3$. The limiting case of $k \to 0$ $(-)$ is shown together with finite values $(\cdots)$. The latter are given for values of $k = 0.07, 0.14, 0.21$, and 0.28. The finite values of k decrease towards the solid line.

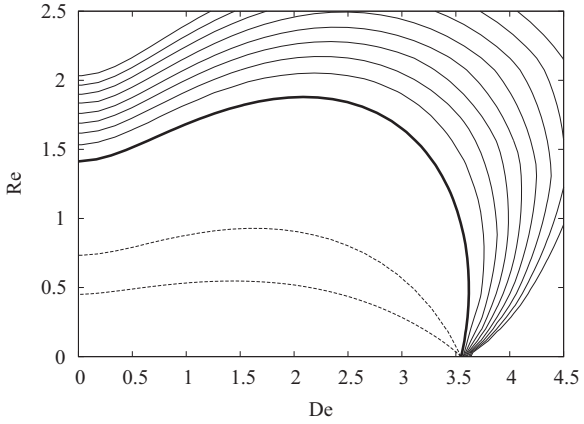

FIG. 4. Growth rate in the Re-De plane with $\Gamma \equiv \mathrm{De}$ and $n = 1.3$. Here, positive $(-)$ and negative $(\cdots)$ growth rate is shown together with the marginal curve (thick line). The contour spacing is 0.01.

the maximum is found) above which a rapid decrease to zero is observed. This behavior is remarkably close to what has been observed in Ref. [9] for a viscoelastic flow simulated by the Oldroyd-B model. The model with $\Gamma \equiv \mathrm{De}$ thus seems to capture viscoelastic behavior of rheopectic fluids.

For thixotropic or shear-thinning cases ($n < 1$) one can easily exclude the emergence of network instabilities by means of the following simple considerations. Large values of a in Eq. (3) correspond to large values of λ which, from Eq. (4), cause an apparent viscosity $\mu = 0$ (or $\mu = \mu_\infty$ if one does not take $\mu_\infty \sim 0$ as in the present study). Under this condition one thus recovers the Newtonian limit, with μ_∞ replacing μ_0. The Newtonian regime is also trivially reached in the opposite limit $a \to 0$. In both limits no network instabilities are thus expected, a fact that can be reasonably extrapolated to all values of a. Although not reported in the present paper, our stability analysis confirms this simple expectation also for finite values of τ.

When considering the solution of the stability problem in the vicinity of the marginal curve, the most unstable perturbation turned out to be large-scale with respect to the basic flow and, furthermore, to have zero phase velocity. The fact that it is large scale will be exploited in Sec. V to obtain perturbative predictions for the marginal curves.

A more general picture of the stability characteristics can be obtained by evaluating the phase velocity, growth rate, and corresponding wave number also in the rest of the parameter space. Such analysis has been performed for the case of $\Gamma \equiv \mathrm{De}$ and $n = 1.3$ by computing the least stable solution, over all possible wave numbers $k \geqslant 0$ in the Re-De plane. In Fig. 3 the wave number for the least stable solution is reported. In the vicinity of the marginal curve the least stable solution is obtained for $k \to 0$, and this holds true also in the stable region. A finite value of k is instead found in the unstable region with increasing value moving away from the marginal curve. It was further found that the phase velocity is zero for both stable and unstable solutions. The growth rate of the results reported in Fig. 3 is shown in Fig. 4. In the stable region the variation of the growth rate is low; on the contrary in the unstable region the growth rate increases rapidly moving away from the marginal curve. This is enhanced as the Reynolds number is decreased. In the vicinity of zero Reynolds number, close to the marginal curve, the growth rate increases rapidly as De is increased indicating a large sensitivity of the stability characteristics with respect to De.

Moreover, considering three-dimensional spanwise periodic perturbations for the cases analyzed here it was found that the least stable solution was always two dimensional. Finally, a general observation regarding the shape of the least stable disturbances, independently of the value of the parameters Re, De, and Γ, is that the vertical velocity component remains constant unlike the other components. A quantification regarding the onset of the instabilities in terms of interaction with the basic flow is considered in Sec. IV by analyzing the energy equation for the linearized system.

IV. ENERGETIC CONSIDERATIONS

In this section we address the emergence of network instabilities in terms of the energy equation for the velocity perturbation. This latter equation follows from Eqs. (7) and (8). Multiplying both sides of Eq. (8) by w_α, averaging over the periodicity box (an operation denoted by brackets) and exploiting the solenoidal condition (7) one obtains

$$\partial_t E = -\langle w_\alpha w_\beta \partial_\beta U_\alpha \rangle - 2\,\langle \mu_b\, e'_{\alpha\beta} e'_{\alpha\beta} \rangle - 2\,\langle \mu' E_{\alpha\beta} e'_{\alpha\beta} \rangle, \tag{12}$$

where $E = \frac{1}{2}\langle w_\alpha w_\alpha \rangle$. All divergence terms, once averaged, are identically zero due to the periodic boundary conditions.

From the above equation one recognizes the production term (first term on the right-hand side), the viscous dissipation (second term on the right-hand side) and, finally, the new term originated from the contribution of the network to the fluid kinetic energy.

In the purely Newtonian case, instabilities appear when the production term becomes negative and overcomes viscous dissipation. In the present non-Newtonian case the situation is more complicated and follows from a detailed balance between production, viscous dissipation, and the contribution from the network.

We first explore the case $\mathrm{De} = 0$ corresponding to an instantaneous reaction of the network to shear. Equation (9) reduces to

$$\sigma = 8\Gamma^2 E_{\alpha\beta} e'_{\alpha\beta}, \tag{13}$$

and the second of Eqs. (11) becomes

$$\mu' = \frac{4\Gamma^2(1+\Lambda)^{\frac{n-3}{2}}(n-1)E_{\alpha\beta}e'_{\alpha\beta}}{\mathrm{Re}}. \tag{14}$$

Inserting Eq. (14) into the third term of Eq. (12), one obtains

$$\langle \mu' E_{\alpha\beta} e'_{\alpha\beta}\rangle = \frac{\langle 4\Gamma^2(1+\Lambda)^{\frac{n-3}{2}}(n-1)E_{\alpha\beta}\ e'_{\alpha\beta}E_{rs}\ e'_{rs}\rangle}{\mathrm{Re}}, \tag{15}$$

which shows, because of its positive sign, the absence of network-induced instabilities for shear-thickening fluids (i.e., $n > 1$). Interestingly, the above quantity is negative for $n < 1$ (i.e., for shear-thinning fluids). In these cases, however, both viscous dissipation and production turned out to act to stabilize possible instabilities induced by the network. These results quantitatively confirm our main claim that a finite-time network response is the crucial ingredient for instabilities in the relevant limit of vanishing inertia to emerge.

To better understand the physical mechanism at work in rheopectic fluids when instabilities for vanishing inertia are triggered, let us move to the Lagrangian view of Eq. (9). For large Γ and De such an equation can be integrated along the characteristics [defined by $\dot{\boldsymbol{y}}(\tau) = \boldsymbol{U}(\boldsymbol{y}(\tau))$] to obtain

$$\sigma(\boldsymbol{x},t) = \sigma(\boldsymbol{x},0) - \\ + 4\Gamma^2 \int_0^t w_\alpha(\boldsymbol{y}(\tau),\tau)\partial_\alpha \left[E_{ab}(\boldsymbol{y}(\tau))E_{ab}(\boldsymbol{y}(\tau))\right] d\tau, \tag{16}$$

where $\boldsymbol{x} = \boldsymbol{y}(t)$. The integral in Eq. (16) represents the sum of the base-flow squared strain-rate variations along the Lagrangian trajectories, built with velocity perturbations alone, measured along the characteristics of the base flow. The crucial difference with respect to the shear-thickening case (where the sign of μ' coincides with that of $E_{\alpha\beta}e'_{\alpha\beta}$ with the result that the network reduces the fluid kinetic energy) is that now $\sigma(\boldsymbol{x},t)$ [and thus $\mu'(\boldsymbol{x},t)$ as it follows from the second of Eqs. (11)] can be either positive or negative depending on the past evolution of the base-flow squared strain rate. Network instabilities arise when, for a given sign of $E_{\alpha\beta}(\boldsymbol{x})e'_{\alpha\beta}(\boldsymbol{x},t)$, μ' acquires the opposite sign.

Although a similar mechanism might work also in the thixotropic case, from our previous analysis both viscous dissipation and the classical production term are always able to stabilize possible instabilities induced by the network.

Let us now continue our analysis focusing on the different contributions in Eq. (12). Because all terms in Eq. (12) are real and involve products of perturbations, the temporal structure of each term is proportional to $\exp[2k\mathrm{Im}(c)t]$. Prefactors in front of each term is a number (i.e., time independent) and its sign determines if the contribution stabilizes or destabilizes the system. To understand the role of different terms in Eq. (12), the model with $\mathrm{De} = \Gamma = 4$ and $n = 1.3$ has been considered and the Reynolds number is varied from $\mathrm{Re} = 0$ to $\mathrm{Re} = 2.5$. This latter value is larger than the purely hydrodynamic threshold to instability (corresponding to $\mathrm{Re} = \sqrt{2}$). As one can see in Fig. 2, for these parameters instabilities are predicted for all Re. It is now interesting to investigate whether, for different Re, different mechanisms of instability arise. The result of this analysis is reported in Fig. 5, where the contributions to the logarithmic derivative of Eq. (12), $\partial_t E/E$, arising from the three terms on the right-hand side of Eq. (12) are shown.

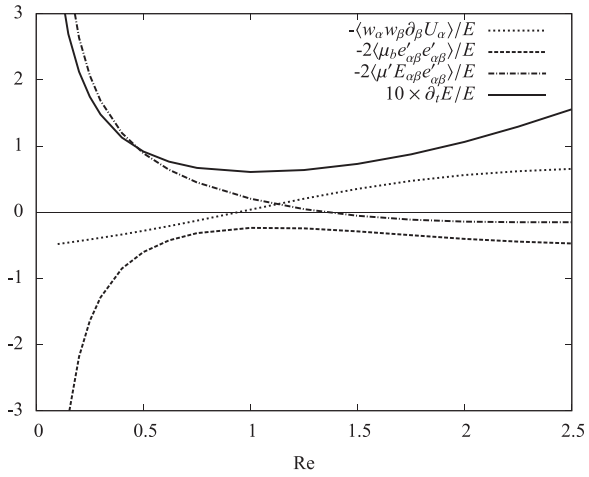

FIG. 5. Energy balance for $\mathrm{De} = \Gamma = 4$ and $n = 1.3$. Along the ordinates we report the different contributions to the total logarithmic derivative, $\partial_t E/E$, from Eq. (12). The symbols represent production $(\cdots)$, dissipation (- -), network (- · -), and total $(-)$, respectively. The last has been scaled by a factor of 10 for readability.

The scenario emerging from this figure can be clearly explained. As expected, for arbitrarily small Re, instability is caused by the term associated with the network. Its contribution becomes smaller and smaller up to a critical Re (of about 1.1 in Fig. 5) above which the classical hydrodynamics term dominates the scene. In this regime, the contribution from the network tends to stabilize the system acting as a sort of enhanced molecular viscosity.

V. MULTIPLE-SCALE EXPANSION

The fact that the most unstable perturbation is on scales much larger than that of the basic flow ($k \ll 1$) suggests the possibility of capturing network instabilities by means of asymptotic perturbative methods. To investigate this possibility, let us denote by ϵ the ratio of small to large scales as the natural perturbative parameter in a multiple-scale expansion [21]. According to this technique, let us introduce a set of slow variables ($\tilde{\boldsymbol{x}} = \epsilon\boldsymbol{x}$, $\tilde{t} = \epsilon^2 t$) in addition to the fast variables $(\boldsymbol{x},t)$ to describe the evolution of the basic flow. The scaling of the slow time $\tilde{t}$ is suggested by physical reasons: we are expecting a diffusive behavior at large scales and the relation between space and time is thus assumed to be quadratic.

The multiple-scale technique [21] treats slow and fast variables as independent in order to capture the secular effects shaping the macroscopic dynamics. The differential operators appearing in Eqs. (7)–(10) transform according to the chain rule as $\partial_i \to \partial_i + \epsilon\tilde{\partial}_i$ and $\partial_t \to \partial_t + \epsilon^2\tilde{\partial}_t$ where $i = 1,2$ denotes x and y and the tilde over the differential operators means differentiation with respect to slow variables. Owing to the linear character of the differential problem (7)–(10) the

field amplitudes can then be rescaled out so that $\phi \equiv (\boldsymbol{w},q,\sigma)$ is expanded as

$$\phi = \phi^{(0)} + \epsilon\phi^{(1)} + \epsilon^2\phi^{(2)} + \cdots, \tag{17}$$

where all functions depend on $(y,t,\tilde{x},\tilde{y},\tilde{t})$ and have the same periodicity as the basic state.

Once Eq. (17) are plugged into Eqs. (7)–(10), the sought large-scale equation emerges from the solvability condition at the second order. In terms of the large-scale stream function defined by the relationships

$$\left\langle w_x^{(0)} \right\rangle = \tilde{\partial}_y \Psi, \quad \left\langle w_y^{(0)} \right\rangle = -\tilde{\partial}_x \Psi, \tag{18}$$

where brackets denote averages over the periodicity box, the large-scale equation has the diffusive form

$$\tilde{\partial}_t \partial^2 \Psi = \nu_{\alpha\beta} \tilde{\partial}_\alpha^2 \tilde{\partial}_\beta^2 \Psi, \tag{19}$$

where $\nu_{\alpha\beta}$ is the so-called eddy-viscosity tensor [22]. Unlike what happens for a passive scalar [23–25], here the eddy viscosity can be either positive or negative definite (see, e.g., Ref. [26] for a relevant example of negative eddy viscosity for Newtonian fluids). Negative eddy viscosity is the fingerprint of large-scale instabilities.

The problem here is thus reduced to study the sign of the operator $\nu_{\alpha\beta}\tilde{\partial}_\alpha^2\tilde{\partial}_\beta^2$, a fact that can be easily done in Fourier space. To do so, let us define θ to be the angle between the perturbation and the basic flow. Longitudinal perturbations correspond to $\theta = 0$ while transverse perturbations correspond to $\theta = \pi/2$. The stability of the system is obtained when $As^2 + Bs + C = 0 \ \forall\, s \geqslant 0$ where $s = \tan^2\theta$ and the coefficients A, B, and C are nontrivial functions of Γ, Re, De, and n. Their expressions are long and do not add any particular information and will therefore be reported elsewhere. We wish to point out that to obtain these coefficients we performed a (regular) perturbative expansion for small Γ, here up to the fourth order. The level of accuracy of the two combined expansions, the multiple-scale expansion, and the small-Γ expansion, can be seen in the right-hand part of Fig. 1 in the parameter space Re-De for $\Gamma = 0.3$ and $n = 1.3$. The agreement between the perturbative prediction (open circles) and that from the numerical strategy (continuous line) is excellent: the multiple-scale expansion thus correctly captures network instabilities.

VI. CONCLUSIONS

A class of purely non-Newtonian instabilities originated by the finite-time response to shear of an underlying non-Newtonian fluid has been investigated both analytically, by means of multiple-scale expansions, and numerically by solving the eigenvalue problem associated with the linear stability analysis of the system.

The main result was the identification of the key physical character a general non-Newtonian fluid has to posses to trigger instabilities even for arbitrarily small fluid inertia. A fluid must react to shear variations in a finite time (compared to the hydrodynamic time scale). Furthermore, the change of viscosity induced by shear variations must be as in rheopectic fluids, i.e., viscosity must increase for increasing shear and this change must occur in a finite time. In this respect, both shear-thinning and shear-thickening fluids do not have the right properties to trigger instabilities arbitrarily close to zero Reynolds number. Their adjustment time to shear variations indeed occur almost instantaneously (i.e., De ~ 0). The same holds true also for thixotropic fluids. The reaction time is finite in this case as for rheopectic fluids but an increasing shear is here associated with a high-to-low transition in the viscosity. As shown by the present analysis, this latter property does not allow instability at vanishing inertia to emerge.

It also clearly emerges that geometry (i.e., phenomena of alignment of the network with the flow) does not play any role here. The network indeed manifests its effects via a scalar field and not via a tensor field as, for example, in the Oldroyd-B model for polymer transport.

Our findings call for numerical investigations and experiments on the deeply nonlinear stage, both for the Kolmogorov flow and for more realistic flow configurations: a natural and speculative question indeed arises on the possible existence of enhanced mixing regime that we can dub "network turbulence." The possible existence of this regime is of paramount importance in microfluidic devices to generate mixing otherwise impossible for Newtonian fluids due to negligible inertia. Our fluid model applies to the class of rheopectic fluids, not necessarily viscoelastic. Our results call for fundamental research in the field of smart materials to synthesize optimal fluid solutions highlighting the rheological properties responsible for the instability mechanism here identified.

ACKNOWLEDGMENTS

Authors thank Alessandro Bottaro and Luca Brandt for useful discussions and suggestions.

[1] P. Tabeling, *Introduction to Microfluidics* (Oxford University Press, Oxford, 2005).
[2] R. C. Anderson, G. J. Bogdan, A. Puski, and X. Su, Genetic analysis systems: Improvements and methods, in *Proc. Solid-State Sens. Actuator Workshop* (IEEE, Hilton Head, SC, 1998), pp. 7–10.
[3] S. Haward, T. Ober, M. Oliveira, M. A. Alves, and G. H. McKinley, Soft Matter **8**, 536 (2012).
[4] R. G. Larson, E. S. G. Shaqfeh, and S. J. Muller, J. Fluid Mech. **218**, 573 (1990).
[5] A. Groisman and V. Steinberg, Nature (London) **405**, 53 (2000).
[6] G. H. McKinley, P. Pakdela, and Öztekinb, J. Non-Newtonian Fluid Mech. **67**, 19 (1996).
[7] P. Pakdel and G. H. McKinley, Phys. Rev Lett. **77**, 2459 (1996).
[8] E. Shaqfeh, Annu. Rev. Fluid Mech. **28**, 129 (1996).
[9] G. Boffetta, A. Celani, A. Mazzino, A. Puliafito, and M. Vergassola, J. Fluid Mech. **523**, 161 (2005).

[10] A. Bistagnino *et al*., J. Fluid Mech. **590**, 61 (2007).
[11] S. Berti, A. Bistagnino, G. Boffetta, A. Celani, and S. Musacchio, Phys. Rev. E **77**, 055306(R) (2008).
[12] B. Toms, Proc. First International Congress on Rheology **2**, 135 (1949).
[13] G. Boffetta, A. Celani, and A. Mazzino, Phys. Rev. E **71**, 036307 (2005).
[14] J. Mewis and N. J. Wagner, Adv. Colloid Interface Sci. **147–148**, 214 (2009).
[15] R. Bird, R. Armstrong, and O. Hassager, *Dynamics of Polymeric Liquids* (Wiley, New York, 1987).
[16] J. Delhommelle and J. Petravic, J. Chem. Phys. **123**, 074707 (2005).
[17] A. Deshpande, J. Krishnan, and P. Sunil Kumar, *Reology of Complex Fluids* (Springer, New York, 2010).
[18] T. Osswald and G. Menges, *Material Science of Polymers for Engineers* (Hanser Gardner Publications, New York, 2003).
[19] V. Arnold and L. Meshalkin, Uspekhi Mat. Nauk **15**, 247 (1960).
[20] J. H. Wilkinson, Lin. Alg. Appl. **28**, 285 (1979).
[21] A. Bensoussan, J.-L. Lions, and G. Papanicolaou, *Asymptotic Analysis for Periodic Structures* (North-Holland, New York, 1978).
[22] B. Dubrulle and U. Frisch, Phys. Rev. A **43**, 5355 (1991).
[23] L. Biferale, A. Crisanti, M. Vergassola, and A. Vulpiani, Phys. Fluids **7**, 2725 (1995).
[24] A. Mazzino, Phys. Rev. E **56**, 5500 (1997).
[25] A. Mazzino, S. Musacchio, and A. Vulpiani, Phys. Rev E **71**, 011113 (2005).
[26] S. Gama, M. Vergassola, and U. Frisch, J. Fluid. Mech. **260**, 95 (1994).